

Article

Effects of Surface Size and Shape of Evaporation Area on SiC Single-Crystal Growth Using the PVT Method

Yu Zhang ¹, Xin Wen ¹, Nuofu Chen ^{1,*}, Fang Zhang ¹, Jikun Chen ² and Wenrui Hu ³

¹ School of New Energy, North China Electric Power University, Beijing 102206, China; 120212211055@ncepu.edu.cn (Y.Z.); 120202111010@ncepu.edu.cn (X.W.); 120212111004@ncepu.edu.cn (F.Z.)

² School of Materials Science and Engineering, Beijing University of Science and Technology, Beijing 100083, China; jikunchen@ustb.edu.cn

³ Institute of Mechanics, Chinese Academy of Sciences, Beijing 100190, China; wrhu@imech.ac.cn

* Correspondence: nfchen@ncepu.edu.cn

Abstract: Silicon carbide (SiC) polycrystalline powder. As the raw material for SiC single-crystal growth through the physical vapor transport (PVT) method, its surface size and shape have a great influence on growth of crystal. The surface size and shape of the evaporation area filled with polycrystalline powder were investigated by numerical simulation in this study. Firstly, the temperature distribution and deposition rate distribution for the PVT system were calculated by global numerical simulation, and the optimal ratio of polycrystalline powder surface diameter to seed crystal diameter was determined to be 1.6. Secondly, the surface of the evaporation area filled with polycrystalline powder was covered by a graphite ring and a graphite disc, respectively, to change its surface shape. The results show that adjusting the surface size and shape of the evaporation area filled with polycrystalline powder is an effective method to control the growth rate, growth stability, and growth surface shape of the single crystal. Finally, the result obtained by selecting appropriate covered structures for actual growth indicates that this process can act as a reference for improving the quality of single crystals.

Keywords: numerical simulation; SiC; single crystal growth; heat transfer; fluid flow



Citation: Zhang, Y.; Wen, X.; Chen, N.; Zhang, F.; Chen, J.; Hu, W. Effects of Surface Size and Shape of Evaporation Area on SiC Single-Crystal Growth Using the PVT Method. *Crystals* **2024**, *14*, 118. <https://doi.org/10.3390/cryst14020118>

Academic Editors: Ikai Lo and Ludmila Isaenko

Received: 22 November 2023

Revised: 12 January 2024

Accepted: 22 January 2024

Published: 25 January 2024



Copyright: © 2024 by the authors. Licensee MDPI, Basel, Switzerland. This article is an open access article distributed under the terms and conditions of the Creative Commons Attribution (CC BY) license (<https://creativecommons.org/licenses/by/4.0/>).

1. Introduction

SiC single crystals are a kind of material with broad development prospects. In recent years, SiC has evolved from a high-potential wide bandgap semiconductor to a widely used material in important fields such as power electronics, 5G communications, renewable energy, rail transit, electric vehicles, aerospace, and other fields [1]. Its excellent physical properties, such as high temperature resistance, high voltage resistance, radiation resistance, and high thermal conductivity, make SiC an indispensable substrate material for energy-saving applications at the electronic device and system level [2]. Its low cost, large size, and the fact that it is defect-free are the biggest challenges for growing SiC single crystals [3]. At present, the PVT growth system has proven to be suitable for SiC crystal growth [4]. The growth of SiC single crystals via the PVT method occurs when heated in a medium-frequency induction furnace and grown in a closed graphite crucible. The elements Si and C are sublimed from the SiC polycrystalline powder and transported to the SiC seed crystal at the top of the crucible for deposition and growth. The temperature during the whole growth process is over 2200 °C. Many different physical and chemical reactions are involved in the deposition and growth processes, including the sublimation of SiC polycrystalline powder, the reaction of meteorological components with the side wall of the crucible, and the final reaction deposition of SiC single crystals at the seed crystal [5,6].

In practice, growing SiC single crystals with large diameters and few defects has been a very difficult task; with the increase in SiC single-crystal size, various possible defects, such as dislocations, stacking faults, point defects, etc., increase exponentially in likelihood [7,8].

Many researchers and teams have conducted various studies on the sublimation process of high-quality SiC single crystals grown using the PVT method. Gao et al. [9] found that controlling the temperature field and moving the graphite crucible upwards during the sublimation process of SiC powder can optimize the temperature gradient of the growth interface, reduce defects, stabilize polytypes, and thus improve the quality of single crystals. Müller et al. [10] found that SiC powder exhibits significant non-uniformity in temperature distribution and investigated the relationship between the growth rate of SiC single crystals and the growth time, as well as the limitations of heat transfer inside the crucible. Furthermore, numerous researchers have exerted themselves to enhance the crucible structure's performance in packaging SiC polycrystalline powder. Wang et al. [11] optimized the single-crystal growth model of the SiC PVT method by studying SiC powders with different particle sizes, and improved the gas phase sublimation rate by changing the surface structure of SiC powder. Kitou et al. [12] fitted conduits in crucibles and found this to be beneficial for obtaining high-quality crystals. Chen et al. [13] investigated the relationship of the distance between SiC powder and the seed crystal, the angle between the upper surface of SiC powder and the crucible wall, and the bending degree of the SiC powder surface with the growth rate, and found that the curved SiC powder surface had a positive effect on the single-crystal growth rate. Much work has been conducted by many teams on the sublimation process of SiC polycrystalline powder and on the optimization of the crucible structure. However, there is currently a lack of studies on design and optimization for the surface size and shape of polycrystalline powder.

Numerical simulation has been widely used in the calculation and simulation of crystal growth to simulate the temperature field, electromagnetic field, and flow field within the growth system, where the output temperature gradient can calculate the mass transfer and stress distribution, which can effectively provide strong support for the optimization of the crystallization process [14]. In addition, existing detection methods face difficulties in real-time observation of the growth inside graphite crucibles. Moreover, the growth cycle of SiC single crystals is long, and the cost is high. Therefore, the growth of SiC single crystals was simulated using an axisymmetric global numerical model [15,16]. Through simulation experiments, the internal related physical field distribution was visualized. According to the structure and mechanism of the SiC single-crystal promotion system grown using the PVT method, the mathematical model of the physical field was established, the boundary conditions were set, the grid was completed, and the multi-field coupling numerical simulation system was constructed using finite element software. The effects of the surface size and shape of polycrystalline powder on the growth of single crystals was explored using the magnetic field, temperature field, and flow field coupling model. Therefore, we investigated the effects of the surface size and shape of polycrystalline powder on single-crystal growth. Firstly, the effects of ratio of polycrystalline powder diameter to seed diameter on crystal growth were discussed, and the optimal ratio was determined. Then, after adopting the optimal ratio, the surface of polycrystalline powder was covered by a graphite ring and a graphite disc, respectively, to change its surface shape. The temperature field and flow field distribution of the optimized growth system were calculated. The effect of adding cover on the polycrystalline powder surface on the growth space was analyzed. In the end, the optimal ratio of polycrystalline powder diameter to seed diameter was obtained, and the ideal cover ratio of the surface of polycrystalline powder was studied. At last, an ideal coverage structure was selected for actual single-crystal growth and detection.

2. Model and Numerical Methods

The SiC PVT growth reactor, illustrated in Figure 1, consists of various components, including seed, polycrystalline powders, crucible, and induction coils, among others, with a focus on 4-inch SiC single-crystal growth. In a closed graphite crucible, the elements Si and C were sublimated from the SiC polycrystalline powder on the bottom and transported to SiC single crystals at the top of the crucible for crystallization. The specific geometric size of the main part of the growth reactor is shown in Table 1, and modeling was carried

out according to the size. Due to the symmetrical distribution of the growth reactor and its interior, the entire model can be simplified into a quarter geometric model, which can greatly reduce the amount of calculations required for computer numerical simulation. After introducing an intermediate-frequency, alternating current into the induction coil, the constantly changing current generated a corresponding magnetic field in the growth space. The magnetic field induced a current inside the graphite crucible, resulting in joule loss and heat generation. The SiC polycrystalline powder began to undergo thermal decomposition and sublimation at a temperature of more than 2200 °C, forming a temperature gradient between the higher-temperature polycrystalline SiC powder and the lower-temperature top region of the SiC seed crystal. Under the action of the temperature gradient, the relevant gas-phase substances were transported upwards and reacted, and the mixed gas was transported to the surface of SiC seed crystal for reaction to produce high-purity SiC, and then attached and deposited to form SiC single crystals [17].

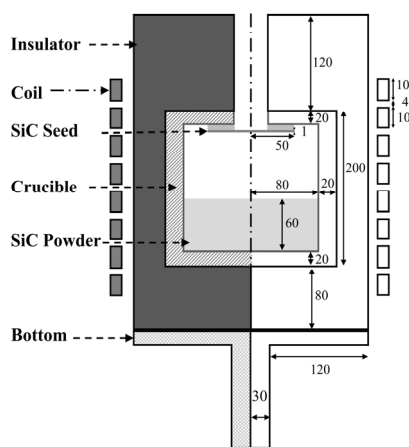


Figure 1. Reactor for 4-inch PVT SiC single-crystal growth (mm).

Table 1. Geometric parameters of growth reactor model (mm).

Part	Size
inner diameter of reactor	150
reactor height	400
insulation thickness	50
inner diameter of growth crucible	80
outer diameter of growth crucible	100
growth crucible height	200
SiC powder thickness	60
SiC seed crystal thickness	1

The following conditions were applied for electromagnetic induction: (1) The system is axisymmetric, and is analyzed in a two-dimensional plane for simulation. (2) All media within the reactor have different linear electrical characteristics in the same direction, which are independent of temperature. The following boundary conditions were applied to heat transfer: (1) Heating chamber is axisymmetric and simulated by a three-dimensional model of a quarter cylinder. (2) The global simulated thermal field of the growth chamber is calculated according to the radiation equation. In addition, in the thermal field analysis, the temperature of the tube wall of the insulation layer was taken as room temperature (23 °C), the surrounding environment was regarded as an absolute black body, and the radiation coefficient of the insulation tube wall was 0.8. Based on the above assumptions, the calculation equation for the coupling of electromagnetic induction and thermal analysis was as follows [18–20]:

$$\nabla \times \left(\frac{1}{\mu_m} \nabla \times A \right) + \varepsilon_m \frac{\partial^2 A}{\partial t^2} + \sigma_c \frac{\partial A}{\partial t} = J_{coil} \quad (1)$$

$$A = \begin{Bmatrix} 0 \\ A_0 e^{i\omega t} + cc \\ 0 \end{Bmatrix}, J_{coil} = \begin{Bmatrix} 0 \\ J_0 e^{i\omega t} + cc \\ 0 \end{Bmatrix} \quad (2)$$

$$\left(\frac{\partial^2}{\partial r^2} + \frac{1}{r} \frac{\partial}{\partial r} - \frac{1}{r^2} + \frac{\partial^2}{\partial z^2} \right) \left(\frac{A_0}{\mu_m} \right) + \varepsilon_m \omega^2 A_0 - i\omega \sigma_c A_0 = -J_0 \quad (3)$$

$$q_{eddy} = \frac{1}{2} \sigma_c \omega^2 A_0 A_0^* \quad (4)$$

$$\nabla \cdot (-k \nabla T) = Q_{th} \quad (5)$$

$$\phi = -k \nabla T \cdot n = h(T - T_{amb}) - \varepsilon \sigma_{st} (T^4 - T_{amb}^4) \quad (6)$$

where μ_m is the magnetic permeability, ε_m is the dielectric constant, σ_c is the conductivity, cc is the complex conjugate; z is the axial coordinate, r is the radial coordinate, and ω is the angular frequency. The boundary condition is $A = 0$, $r = 0$ and $(r^2 + z^2) \rightarrow \infty$; q_{eddy} is the volume density of the generated thermal power; Q_{th} is the heat transfer in the reaction chamber; ϕ is the thermal radiation between the walls (ignoring heat transfer caused by chemical reactions); and T_{amb} is the ambient temperature.

The following conditions were applied to mass transfer: (1) In numerical calculation, the gas phase in the growth space is regarded as an ideal gas, and the diffusion of the growth space can be simplified into a binary diffusion system, which mainly includes two components: ideal gas and shielding gas argon. (2) Due to the growth kinetics, a growth layer, also known as the adsorption layer, is formed on the surface of the seed crystal, and a detachment layer or desorption layer formed by gas phase components is formed on the surface of the SiC polycrystalline powder. When the pressure of the mixed gas at the seed crystal surface is not less than the equilibrium partial pressure, it is more easily adsorbed. In the desorption layer, when the pressure of the mixed gas is not high enough to balance the partial pressure, it will escape and diffuse. (3) The material transfer in the reactor has the most significant impact on the mass transfer rate of the components of the mixed gas phase. Therefore, the impact of the adsorption layer and the desorption layer can be ignored in the calculation process, and only the impact of the material transfer process on the mass transfer density needs to be considered. Based on the above assumptions and Fick's law, the equation for calculating mass transfer is as follows [21]:

$$J_A = \frac{D_{AB} (P_{A(powder)} - P_{A(seed)})}{RT_{avg}L} \quad (7)$$

where J represents the flow rate of mass flow, P represents the equilibrium partial pressure, L is the distance between the seed crystal and SiC polycrystalline powder, T_{avg} represents the average temperature in the growth reactor, $P_{A(powder)}$ represents the surface pressure of SiC polycrystalline powder, $P_{A(seed)}$ represents the surface pressure of the seed crystal, D_{AB} is the diffusion coefficient of the component in the growth reactor, and R is the gas constant.

The following hypothetical conditions were applied to fluid flow: (1) The fluid in the growth chamber is a single fluid. (2) The fluid in the growth chamber is incompressible. (3) The buoyancy effect caused by the temperature gradient needs to be considered in the calculation. Therefore, the equations can be expressed as [22,23]:

$$-v \cdot u + (u \cdot \nabla)u + \nabla P = -\rho' \alpha_v T g \quad (8)$$

$$-\nabla \cdot u = 0 \quad (9)$$

$$G_r = \frac{g\alpha_v\Delta TL^3}{\nu^2} \quad (10)$$

where u represents velocity, P is the pressure, ν is the viscosity coefficient, ρ' is the density of the mixed gas, g is the gravity vector, α_v is the isobaric expansion coefficient of an ideal gas, ΔT is the temperature difference, L is the inner diameter of the crucible, and the Grashof number (G_r) is the ratio of the buoyant force to the viscous force.

3. Results

3.1. Effects of Ratio of Polycrystalline Powder Diameter to Seed Crystal Diameter

Figure 2 shows a cross-sectional diagram of the 4-inch PVT SiC growth crucible, with a two-dimensional coordinate system established at the bottom center of the crucible as the origin. In a closed crucible, the elements Si and C are sublimated from SiC polycrystalline powder on the bottom, then transported to the SiC single crystal on top of the crucible for deposition and growth. The ratio of the diameter of the evaporation area filled with polycrystalline powder to the seed crystal diameter can be expressed as:

$$D = D_{\text{powder}}/D_{\text{seed}} \quad (11)$$

D_{powder} is the diameter of the evaporation area filled with polycrystalline powder; D_{seed} is the seed crystal diameter. Based on the actual situation of crystal growth and the experimentation with controlling variables, the method of adjusting the polycrystalline powder diameter D_{powder} while keeping the seed crystal diameter D_{seed} unchanged was adopted to change the size of D . In addition, the axial temperature gradient needed to be defined as: T_{powder} to T_{seed} ; the radial temperature gradient was also defined as T_{edge} to T_{center} .

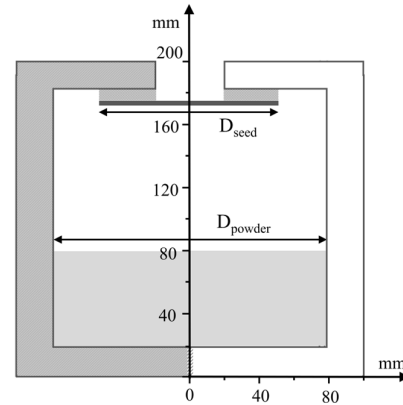


Figure 2. Schematic diagram of the ratio of D_{powder} to D_{seed} in the cross-section of SiC growth crucible.

For the temperature distribution, the axial temperature gradient along the central axis and radial temperature gradient along the seed surface at different values of D are given in Figure 3. As D increased, the axial temperature gradient gradually increased to become stable. The reason for this is that the magnetic induction at the lower part of the reactor was stronger than the magnetic induction at the top of the reactor, resulting in an axial temperature gradient. The heat generated by the sidewall of reactor had a significant influence on axial temperature gradient when D was small. While D increased, the axial temperature gradient was less affected by side heating of the crucible and more affected by heat production at the crucible bottom. When $D > 1.5$, the heat generated by the sidewall of crucible had a low influence on the axial temperature gradient, and the axial temperature gradient remained stable. The heat generated by the side wall of the reactor created a radial temperature gradient. The radial temperature gradient along the seed surface increased monotonically with the increase in D .

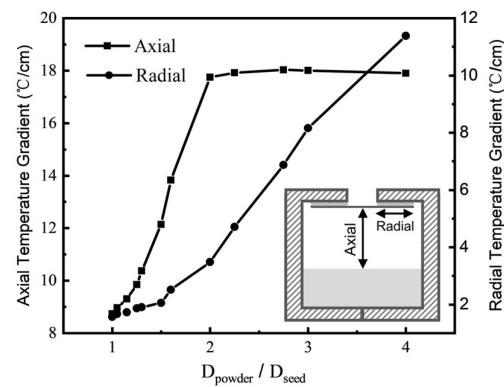


Figure 3. Temperature gradient distribution at different values of D .

Therefore, the temperature field distribution of PVT system can be affected by the ratio of polycrystalline powder diameter to seed crystal diameter. The temperature gradient requirements can be satisfied by appropriate values of D , and high-quality SiC single crystals can be obtained. At $D < 1.5$, low axial temperature gradients led to a lack of power for mass transfer. In the case of $D > 1.7$, the axial temperature gradient was stable, and the radial temperature gradient increased linearly. The thermal stress during single-crystal growth increased with the increasing radial temperature gradient, and crystal defects were easily generated. Therefore, D needs to be limited. According to the results of temperature gradient distribution, $D = D_{\text{powder}}/D_{\text{seed}} = 1.5 \sim 1.7$ is more suitable for SiC single-crystal growth.

For the flow field distribution, the deposition rate along the surface of the seed crystal is given in Figure 4. The crystal growth rate can be reflected by the deposition rate. As D increased, the deposition rate decreased. At $D < 1.5$, the deposition rate of the seed crystal center was lower than that of the edge, the growth surface shape was slightly concave, and crystal defects were easily generated. In the case of $D > 1.5$, the deposition rate of the seed crystal center was higher than that of the edge, and the growth surface shape was slightly convex. Combined with changes in temperature gradient, $D = 1.6 \sim 1.7$ is suitable for SiC single-crystal growth. Among these two options, considering the radial temperature gradient and the micro convexity of the single-crystal growth surface, $D = 1.6$ is the best choice.

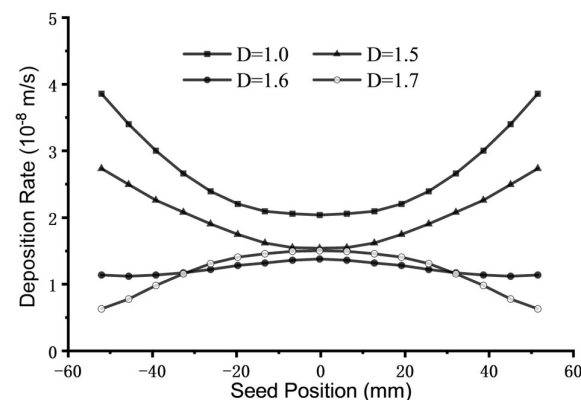


Figure 4. Deposition rate distribution at different values of D .

3.2. Effects of Cover of Polycrystalline Powder Surface

According to the above research results, the effects of the cover on single crystal growth were studied at $D = 1.6$. Two cover methods were investigated. The central part of the surface of the evaporation area filled with polycrystalline powder was covered by a graphite disc. The edge part of the surface of the evaporation area filled with polycrystalline

powder was covered by a graphite ring. The cover was symmetrically distributed, and the cover ratios (R) were $1/5$, $2/5$, $3/5$, and $4/5$, as shown in Figure 5.

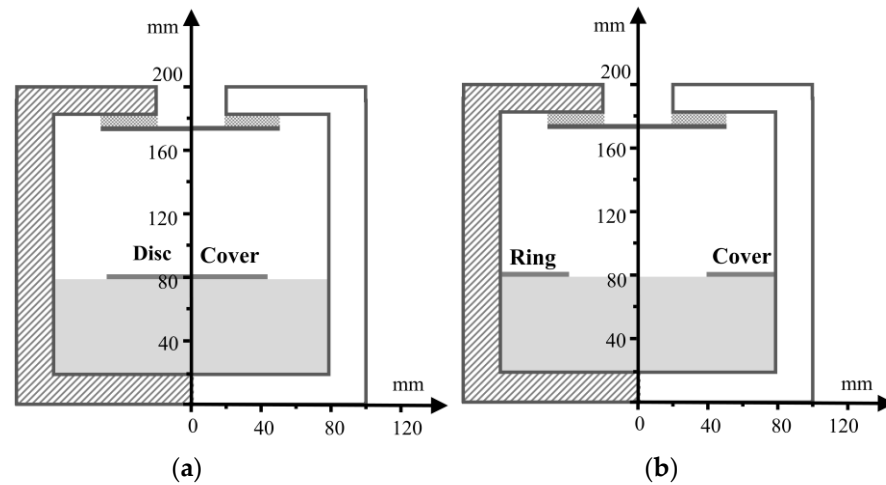


Figure 5. (a) Graphite disc cover, (b) graphite ring cover.

The temperature field of the optimized growth space was analyzed. The temperature gradient distributions at different cover ratios for the case of the graphite disc cover is shown in Figure 6a. The temperature gradient distributions at different cover ratios for the case of the graphite ring cover is shown in Figure 6b. With the graphite disc, as the covered area increased, the axial temperature gradient increased slightly, while the radial temperature gradient gradually decreased. The reason for this is that the heat induced by the graphite disc gradually increased as the graphite disc area increased, thus increasing the axial temperature gradient.

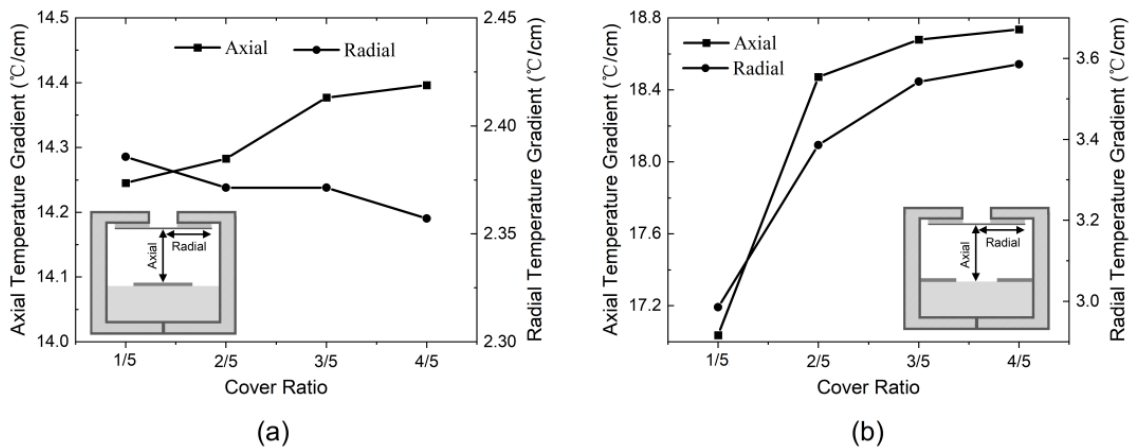


Figure 6. Temperature gradient distribution at different cover ratios: (a) graphite disc cover, (b) graphite ring cover.

The temperature distribution in the growth space was analyzed in the case of the graphite ring cover. As the covered area increased, the axial temperature gradient and radial temperature gradient increased. This is because, as the graphite ring area increased, the temperature of the polycrystalline powder near the crucible wall increased due to the heat induced by the graphite ring, thus increasing the axial temperature gradient and radial temperature gradient.

For the flow field distribution, the deposition rate distribution along the seed crystal in the case of the graphite disc cover is shown in Figure 7a, and the deposition rate distribution

in the case of the graphite ring cover is shown in Figure 7b. The cover ratios (R) were 1/5, 2/5, 3/5, and 4/5.

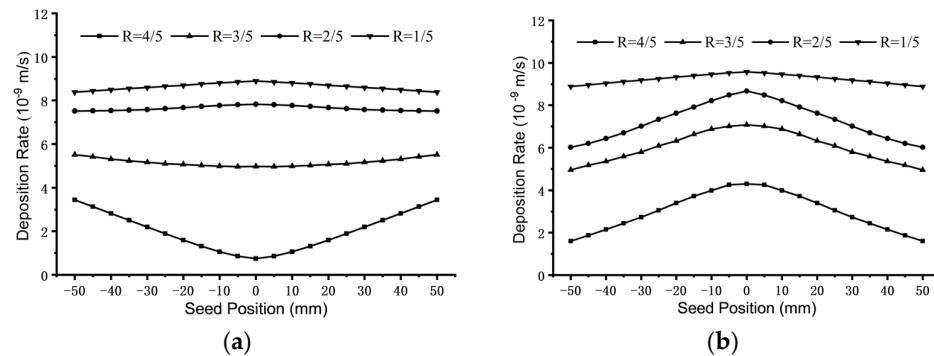


Figure 7. The deposition rate distribution at different cover ratios (R): (a) graphite disc cover, (b) graphite ring cover.

For the graphite disc, the deposition rate decreased as the covered area increased, and the deposition rate at the center decreased more significantly than that at the edge. At cover ratio of less than 2/5, the center deposition rate was high, the edge deposition rate was low, and the crystal surface was slightly convex, making it easy to obtain high-quality single crystals. When the coverage rate was greater than 2/5, the edge deposition rate was higher, while the center deposition rate was lower, and the shape of the crystal growth surface was slightly concave. In combination with the temperature gradient variation of single-crystal growth, the graphite disc cover ratio should be less than 2/5 to better control the shape and quality of the crystal growth.

For the graphite ring, the deposition rate decreased with the increasing covered area. The deposition rate decreased significantly as the cover ratio increased from 1/5 to 2/5. The center deposition rate decreased from 1×10^{-7} m/s to 0.4×10^{-7} m/s in the case of a cover ratio of 4/5, and the mass transfer was significantly affected by the graphite ring cover. Figure 7b shows that both the center and edge deposition rates gradually decreased as the covered area increased, with the center deposition rate remaining consistently higher than the edge deposition rate, while the edge deposition rate had a more pronounced decreasing trend. The growth surface became convex in shape as the difference in deposition rate between the center and the edge increased.

The axial gradient and radial temperature gradient can be changed using a graphite disc or ring to cover the polycrystalline powder surface, thus influencing the process of mass transfer and changing the crystal deposition rate distribution. The two covers, the graphite disc and graphite ring, have different effects on the growth of crystals. As the coverage increases, the difference in deposition rate between center and edge of the seed crystal gradually decreases and increases, respectively.

Finally, according to the simulation results of the structure, temperature field, and flow field of the coverage type combined with the actual situation, it was decided to use a graphite ring with a cover ratio of $R = 1/5$ as the optimized component for the actual growth of SiC single crystals. The final result was a SiC ingot with a diameter of 12 mm and a height of 20 mm, and after processing, the diameter of the SiC wafer was 10 mm and the thickness was 0.3 mm. The SiC ingot obtained via the PVT process, combined with the aforementioned graphite ring covering the SiC polycrystalline powder with a coverage rate of $R = 1/5$ for actual growth, is shown in Figure 8. As can be seen from the figure of the growth ingot, the surface of the grown SiC ingot was relatively flat, without significant fluctuation, and the edge growth of the ingot was also relatively complete, with good overall quality. Then, the sample ingot of SiC was characterized using XRD, and the characterization results of the sample detection are presented in Figure 9. It can be concluded that the grown crystal was a (0004) 4H-SiC single crystal. Therefore, the addition

of a graphite ring with an appropriate proportion results in higher quality and more optimal growth of SiC single crystals, which can play a certain expected optimization role.



Figure 8. PVT SiC ingot obtained by adding $R = 1/5$ graphite ring for an optimized structure.

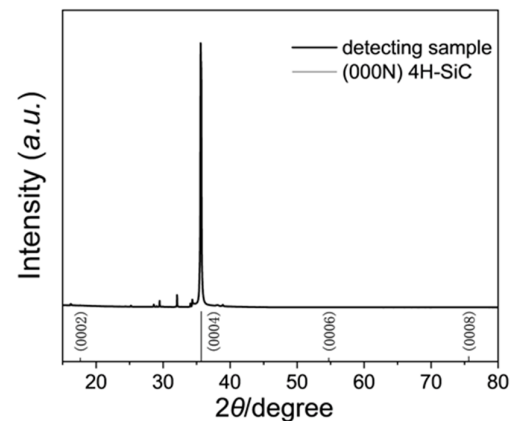


Figure 9. The XRD curves for the detecting sample and standard (000N) of 4H-SiC.

4. Conclusions

A global numerical model was used to calculate the temperature gradient and deposition rate distribution of an SiC single crystal grown using the PVT method. The ratio of the evaporation area filled with polycrystalline powder diameter to the seed diameter and the influence of evaporation area filled with polycrystalline powder surface shape on crystal growth were investigated, and the appropriate shape and size for actual single-crystal growth and characterization were selected.

The optimal cover ratio was researched, combining the temperature gradient and deposition rate distribution. When the ratio of the evaporation area filled with polycrystalline powder diameter to the seed diameter (D) was less than 1.5, the axial temperature gradient was small, leading to a lack of mass transfer power. In addition, the edge deposition rate on the surface of the seed crystal was higher than the center deposition rate; thus, the surface shape was concave, which tends to generate stress and affect the quality of the single crystal. At $D > 1.7$, the radial temperature gradient linearly increased, causing a synchronous increase in thermal stress and increasing the possibility of crystal defects; the surface shape was convex. The results indicate that when $D = 1.6$, the temperature gradient and the slightly convex surface are more suitable for crystal growth.

The influence of two different covers and diverse cover ratios on the crystal growth was researched at $D = 1.6$. When the cover ratio of the graphite disc was less than $2/5$, the central deposition rate was slightly higher than that of the edge. The growth surface was slightly convex, indicating the superior quality of the single-crystal growth. The difference in the

deposition rate between the center and edge of the graphite ring gradually increased as the coverage rate increased, resulting in severe convexity on the growth surface. In summary, the process of mass transfer can be influenced by cover, which alters the distribution of the deposition rate, impacts the surface shape, and affects the uniformity of single-crystal growth. Selecting an appropriate proportion of cover structures allows for more precise growth control and establishes a certain reference value to enhance single-crystal quality.

Author Contributions: Conceptualization, N.C.; methodology, Y.Z. and X.W.; software, Y.Z. and X.W.; validation, Y.Z.; investigation, Y.Z.; resources, Y.Z. and F.Z.; data curation, F.Z.; writing—original draft, X.W.; writing—review & editing, Y.Z.; visualization, X.W.; supervision, N.C., J.C. and W.H.; project administration, N.C. and J.C.; funding acquisition, N.C. All authors have read and agreed to the published version of the manuscript.

Funding: Ministry of Science and Technology of the People’s Republic of China: 2021YFA0718900.

Data Availability Statement: The original contributions presented in the study are included in the article, further inquiries can be directed to the corresponding author.

Conflicts of Interest: The authors declare no conflict of interest.

References

1. Li, J.; Yang, G.; Liu, X.; Luo, H.; Xu, L.; Zhang, Y.; Cui, C.; Pi, X.; Yang, D.; Wang, R. Dislocations in 4H silicon carbide. *J. Phys. D Appl. Phys.* **2022**, *55*, 46. [[CrossRef](#)]
2. Yakimova, R.; Syväjarvi, M.; Iakimov, T.; Jacobsson, H.; Kakanakova-Georgieva, A.; Råback, P.; Janzén, E. Growth of silicon carbide: Process-related defects. *Appl. Surf. Sci.* **2001**, *184*, 27–36. [[CrossRef](#)]
3. Nakamura, D.; Shigetoh, K. Fabrication of large-sized TaC-coated carbon crucibles for the low-cost sublimation growth of large-diameter bulk SiC crystals. *Jpn. J. Appl. Phys.* **2017**, *56*, 85504. [[CrossRef](#)]
4. Tairov, Y.M.; Tsvetkov, V.F. Progress in controlling the growth of polytypic crystals. *Prog. Cryst. Growth Charact.* **1983**, *7*, 111–162. [[CrossRef](#)]
5. Chen, Q.S.; Zhang, H.; Prasad, V.; Balkas, C.M.; Yushin, N.K. Modeling of Heat Transfer and Kinetics of Physical Vapor Transport Growth of Silicon Carbide Crystals. *J. Heat Transf.* **2001**, *123*, 1098–1109. [[CrossRef](#)]
6. Sudarshan, T.S.; Maximenko, S.I. Bulk growth of single crystal silicon carbide. *Microelectron. Eng.* **2005**, *83*, 155–159. [[CrossRef](#)]
7. Lin, S.; Chen, Z.; Yang, Y.; Liu, S.; Ba, Y.; Li, L.; Yang, C. Formation and evolution of micropipes in SiC crystals. *CrystEngComm* **2012**, *14*, 1588–1594. [[CrossRef](#)]
8. Fiscaro, G.; Bongiorno, C.; Deretzis, I.; Giannazzo, F.; La Via, F.; Roccaforte, F.; Zielinski, M.; Zimbone, M.; La Magna, A. Genesis and evolution of extended defects: The role of evolving interface instabilities in cubic SiC. *Appl. Phys. Rev.* **2020**, *7*, 021402. [[CrossRef](#)]
9. Gao, P.; Xin, J.; Liu, X.; Zheng, Y.; Shi, E. Control of 4H polytype of SiC crystals by moving up the crucible to adjust the temperature field of the growth interface. *CrystEngComm* **2019**, *21*, 6964–6968. [[CrossRef](#)]
10. Müller, S.G.; Eckstein, R.; Hofmann, D.; Koelbl, M.; Schmitt, E.; Kadinski, L.; Kaufmann, P. Modelling of the PVT-SiC Bulk Growth Process Taking into Account Global Heat Transfer, Mass Transport and Heat of Crystallization and Results on its Experimental Verification. *Mater. Sci. Forum* **1997**, *352*, 57–60. [[CrossRef](#)]
11. Wang, X.; Cai, D.; Zhang, H. Increase of SiC sublimation growth rate by optimizing of powder packaging. *J. Cryst. Growth* **2007**, *305*, 122–132. [[CrossRef](#)]
12. Kitou, Y.; Bahng, W.; Kato, T.; Nishizawa, S.I.; Arai, K. Flux-Controlled Sublimation Growth by an Inner Guide-Tube. *Mater. Sci. Forum* **2002**, *444*, 83–86. [[CrossRef](#)]
13. Chen, X.J.; Liu, L.J.; Tezuka, H.; Usuki, Y.; Kakimoto, K. Optimization of the design of a crucible for a SiC sublimation growth system using a global model. *J. Cryst. Growth* **2007**, *310*, 1810–1814. [[CrossRef](#)]
14. Steiner, J.; Arzig, M.; Denisov, A.; Wellmann, P.J. Impact of Varying Parameters on the Temperature Gradients in 100 mm Silicon Carbide Bulk Growth in a Computer Simulation Validated by Experimental Results. *Cryst. Res. Technol.* **2020**, *55*, 1900121. [[CrossRef](#)]
15. Ariyawong, K.; Chatillon, C.; Blanquet, E.; Dedulle, J.M.; Chaussende, D. A first step toward bridging silicon carbide crystal properties and physical chemistry of crystal growth. *CrystEngComm* **2016**, *18*, 2119–2124. [[CrossRef](#)]
16. Zhang, S.; Li, T.; Li, Z.; Sui, J.; Zhao, L.; Chen, G. Thermal field design of a large-sized SiC using the resistance heating PVT method via simulations. *Crystals* **2023**, *13*, 1638. [[CrossRef](#)]
17. Zhang, S.; Fu, G.; Cai, H.; Yang, J.; Fan, G.; Chen, Y.; Li, T.; Zhao, L. Design and Optimization of Thermal Field for PVT Method 8-Inch SiC Crystal Growth. *Materials* **2023**, *16*, 767. [[CrossRef](#)]
18. Roy, A.; Mackintosh, B.; Kalejs, J.P.; Chen, Q.S.; Zhang, H.; Prasad, V. A numerical model for inductively heated cylindrical silicon tube growth system. *J. Cryst. Growth* **2000**, *211*, 365–371. [[CrossRef](#)]

19. Su, J.; Chen, X.; Li, Y. Numerical design of induction heating in the PVT growth of SiC crystal. *J. Cryst. Growth* **2014**, *401*, 128–132. [[CrossRef](#)]
20. Chen, Q.S.; Gao, P.; Hu, W.R. Effects of induction heating on temperature distribution and growth rate in large-size SiC growth system. *J. Cryst. Growth* **2004**, *266*, 320–326. [[CrossRef](#)]
21. Chen, Q.S.; Yan, J.Y.; Prasad, V. Application of flow-kinetics model to the PVT growth of SiC crystals. *J. Cryst. Growth* **2006**, *303*, 357–361. [[CrossRef](#)]
22. Pons, M.; Blanquet, E.; Dedulle, J.M.; Garcon, I.; Madar, R.; Bernard, C. Thermodynamic heat transfer and mass transport modeling of the sublimation growth of silicon carbide crystals. *J. Electrochem. Soc.* **2019**, *143*, 3727–3735. [[CrossRef](#)]
23. Chen, H.; Hang, W.; Wang, R.; Yuan, J.; Pi, X.; Yang, D.; Han, X. Numerical analysis of the dislocation density in n-type 4H-SiC. *CrystEngComm* **2023**, *25*, 3718.

Disclaimer/Publisher's Note: The statements, opinions and data contained in all publications are solely those of the individual author(s) and contributor(s) and not of MDPI and/or the editor(s). MDPI and/or the editor(s) disclaim responsibility for any injury to people or property resulting from any ideas, methods, instructions or products referred to in the content.